Applied Radiation and Isotopes 107 (2016) 330–334

Contents lists available at ScienceDirect

Applied Radiation and Isotopes

journal homepage: www.elsevier.com/locate/apradiso

Using a Tandem Pelletron accelerator to produce a thermal neutron beam for detector testing purposes

L. Irazola [a,b,*], J. Praena [c,d], B. Fernández [c], M. Macías [c], R. Bedogni [e], J.A. Terrón [b,a], B. Sánchez-Nieto [f], F. Arias de Saavedra [d], I. Porras [d], F. Sánchez-Doblado [a,b]

[a] *Departamento de Fisiología Médica y Biofísica, Universidad de Sevilla, Spain*
[b] *Servicio de Radiofísica, Hospital Universitario Virgen Macarena, Sevilla, Spain*
[c] *Departamento de Física Atómica, Molecular y Nuclear, Universidad de Granada, Spain*
[d] *Centro Nacional de Aceleradores (US-JA-CSIC), Sevilla, Spain*
[e] *Istituto Nazionale di Fisica Nucleare (INFN), Frascati, Italy*
[f] *Instituto de Física, Pontificia Universidad Católica de Chile, Santiago, Chile*

HIGHLIGHTS

- Monodirectional neutron beam (<1 eV, $\sim 2\times10^3$ cm^{-2} s^{-1}) was tuned up in a 3 MV tandem.
- Reproducibility of the thermal neutron field at test point was estimated in $\pm 4\%$.
- New setup represents a good tool for stability control of neutron detectors.

ARTICLE INFO

Article history:
Received 7 September 2015
Received in revised form
3 November 2015
Accepted 10 November 2015
Available online 11 November 2015

Keywords:
Neutron detectors
Thermal neutrons
TNRD
Pelletron

ABSTRACT

Active thermal neutron detectors are used in a wide range of measuring devices in medicine, industry and research. For many applications, the long-term stability of these devices is crucial, so that very well controlled neutron fields are needed to perform calibrations and repeatability tests. A way to achieve such reference neutron fields, relying on a 3 MV Tandem Pelletron accelerator available at the CNA (Seville, Spain), is reported here. This paper shows thermal neutron field production and reproducibility characteristics over few days.

1. Introduction

Achieving stable thermal neutron beams for calibrating and testing thermal neutron detectors is an important challenge in a number of fields where ionizing radiations are employed. Traditionally, metrology-grade thermal neutron fields are obtained by moderating radionuclide sources of ^{252}Cf or ^{241}Am–Be, with large polyethylene or graphite blocks. An example is the SIGMA facility of IRSN France (Muller et al., 2003; Lacoste, 2007). However, most of the existing facilities were decommissioned because their internal sources were too old to guarantee a safe operation. In addition, achieving large radionuclide sources for new facilities has became unfeasible for both economical and safety reasons. As a consequence, the scientific community is searching for alternative sources of thermal neutron fields. Exploiting the ^{7}Li(p,n) reaction at near-threshold proton energies is a good option because established nuclear data are available and very low-energy neutrons can be achieved, thus requiring very reduced amount of additional thermalizing material.

The 3 MV Tandem Pelletron[1] accelerator (Praena et al., 2013) at CNA (Centro Nacional de Aceleradores, Sevilla, Spain) was used for this purpose. Some sheets of lead were added to reduce the photon field and a few cm of thick polyethylene moderator was adopted as moderator.

* Corresponding author at: Departamento de Fisiología Médica y Biofísica, Universidad de Sevilla, Spain.
E-mail address: leticia@us.es (L. Irazola).

[1] http://www.pelletron.com/negion.htm

http://dx.doi.org/10.1016/j.apradiso.2015.11.020
0969-8043/

The field was monitored, over three days of operation, using (a) a proton current integrator connected to the target backing, and (b) the active thermal neutron detector called *TNRD* (Thermal Neutron Rate Detector) (Bedogni et al., 2014), used in medical physics (Irazola et al., 2014; 2015b) to estimate neutron equivalent doses to peripheral organs for oncological patients treated with medical accelerators (Expósito et al., 2013), using the methodology established by Sánchez-Doblado et al., 2012, Gómez et al., 2010 and Romero-Expósito et al., 2015.

2. Material and method

2.1. TNRD neutron detector

Fig. 1 shows the *TNRD* detector, developed by INFN-LNF, Italy (Bedogni et al., 2014). This detector is based on a low-cost commercial solid-state device sensitized to thermal neutrons through a customized physical–chemical treatment. Its active area is 1 cm^2 and the overall dimensions are approximately $1.5 \times 1 \times 0.4$ cm^3. It linearly responds in terms of thermal neutron fluence rate from 10^2 up to 10^6 $cm^{-2}\,s^{-1}$. *TNRD* signal is amplified in a low-voltage electronics module and sent to a PC-controlled programmable ADC. Control software was developed in LabView© (2010 National Instruments). *TNRD* output is a DC voltage directly proportional to the thermal neutron fluence rate. Every *TNRD* is individually calibrated. The accuracy of the detector is within $\pm$5%, or better, for the fluence rate interval from 500 up to 10^6 $cm^{-2}\,s^{-1}$ (Bedogni et al., 2014). Additional uncertainty terms should be added, in practical measurements, if the neutron field has unknown direction distribution and is superposed to an intense gamma component. The parasitic response of *TNRD* to photons has been additionally evaluated (Terrón et al., 2015; Irazola et al., 2015a,c). The reproducibility of *TNRD*, previously assessed using a constant thermal field from a moderated ^{241}Am–Be source, is $\pm$1.2% over a time interval of days.

2.2. Neutron spectrum determination

The ^{7}Li(p,n)^{7}Be reaction has been studied in terms of total neutron yield, energy and angle distribution of the secondary neutrons as a function of the target thickness and projectile energy (Yu et al., 1998; Lederer et al., 2012). A FORTRAN code was written to generate the angle – and energy – distribution of neutrons based on analytical description of experimental data (Lee and Zhou, 1999). MCNPX (v2.5) (Pelowitz, 2005) was used for their transport. ENDF/B-VII.0 and ENDF/B-VI were used for particle-production and transport data and photoatomic data, respectively. The neutron spectra generated by ^{7}Li(p,n)^{7}Be at 1912 keV, which is used in the present experiment, was successfully modeled previously by Praena et al. (2013). The method of modelization, FORTRAN code for generation and MCNPX for transport, was also checked with neutron spectra emitted at different angles by the ^{7}Li(p,n)^{7}Be reaction near-threshold, Praena et al. (2014). MCNPX was also used to determine the optimal thickness of lead needed to reduce the parasitic photon field, due to the 477 keV photons from ^{7}Li(p,n)^{7}Be reaction. This value was fixed to 2.55 cm (17 lead sheets of 1.5 mm each), located 0.4 cm after the target. To thermalize the field, an optimized 2.2 cm thick polyethylene sheet was added immediately after the lead. Lateral size of both pieces was 20×20 cm^2. *TNRD* detector was then placed in an aluminum support 3.5 cm after the polyethylene block (Praena et al., 2015). This is the conventional point of test. The complete setup is shown in Fig. 2.

Fig. 3a shows simulated angle-integrated primary neutron spectrum at source position while Fig. 3b displays the simulated neutron spectrum at detector position. It can be noticed that only neutrons of energy below 1 eV reach *TNRD*. Neutron spectra were obtained with a MCNP tally 4 which calculates de flux (n/cm^2) averaged over the lithium target (a) *TNRD* detector (b) normalized to total number of neutrons generated in the simulation.

Fig. 1. One of the *TNRD* detectors (marked with a white box) and associated six electronics channels.

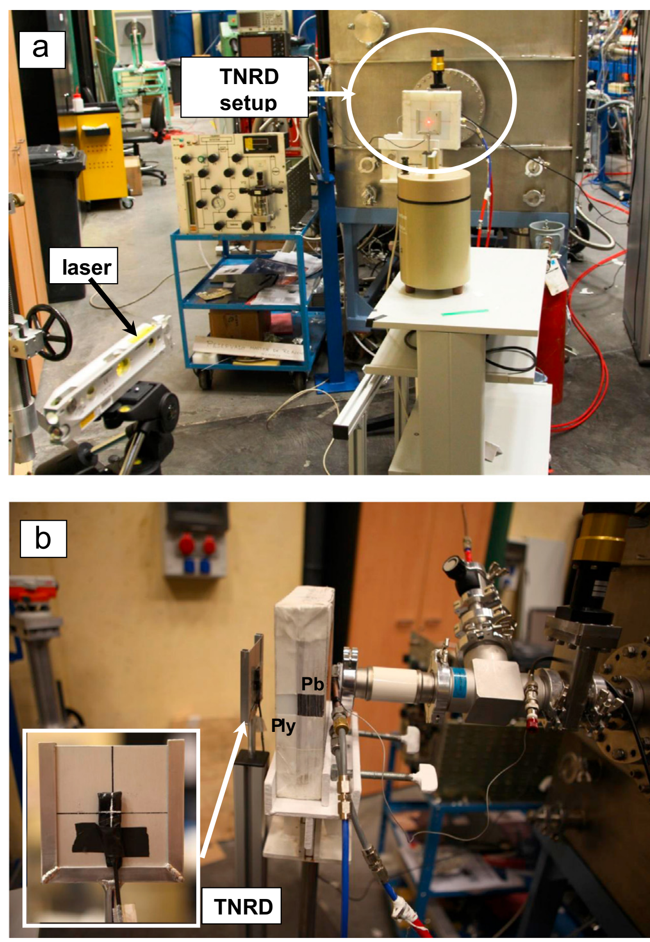

Fig. 2. (a) Experimental setup aligned following the lithium target by using a fixed laser. (b) Detail of *TNRD* setup consisting on: a 2.55 cm lead layer and a 2.2 cm polyethylene (Ply) layer (both of 20×20 cm^2) located between the lithium target and the detector (distance of approximately 8.9 cm). Inset shows *TNRD* location in the aluminum support.

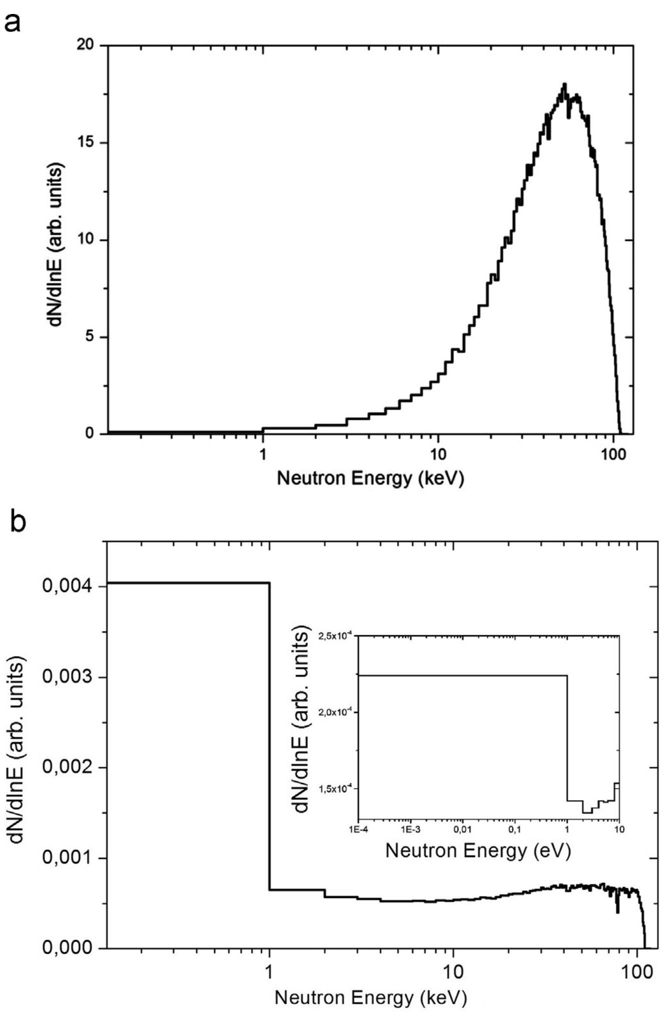

Fig. 3. (a) Simulated neutron unitary spectrum: (a) at source position with ^{7}Li(p,n) reaction at $E_p = 1912$ keV and (b) at *TNRD* position using 2.2 cm polyethylene and 2.55 cm lead filters. Inset shows how the majority of neutrons below 1 keV have an energy lower than 1 eV.

2.3. Proton accelerator and target

The neutron beam was obtained from the CNA 3 MV Tandem Pelletron accelerator at 917 kV nominal voltage. Fig. 4a shows the final part of the Basic Nuclear Physics (FNB) Tandem accelerator line, used in this experiment. It consists on a vacuum pipe housing a copper backing as cooling system. This backing holds a 50 µm thickness aluminum foil and the lithium target layer. The dimensions of this piece are 3x3 × 0.8 cm^3 with a centered cylinder hole of 1 cm of diameter and 0.75 cm height, used to place the lithium layer (380 µm thickness). To prevent target melting, the copper support contains an internal cooling water circuit. Proton current on the lithium target was measured by connecting the copper backing to an Ortec Digital Current Integrator (Model 439). The nominal reproducibility of the electrometer is ± 0.01%. Proton current could be varied up to about 2 µA, corresponding to a thermal neutron fluence of about 2500 cm^{-2} s^{-1} at the point of test.

To prevent non-target contributions to the measured proton current, a double collimator system consisting of two rings, one in copper and the other in Teflon® (connected through two ceramic screws, as shown in Fig. 4b), was used. Collimators and target holder have external diameter of 3 cm. Internal diameter is 1.1 cm for copper ring and 1 cm for Lithium target and Teflon® ring.

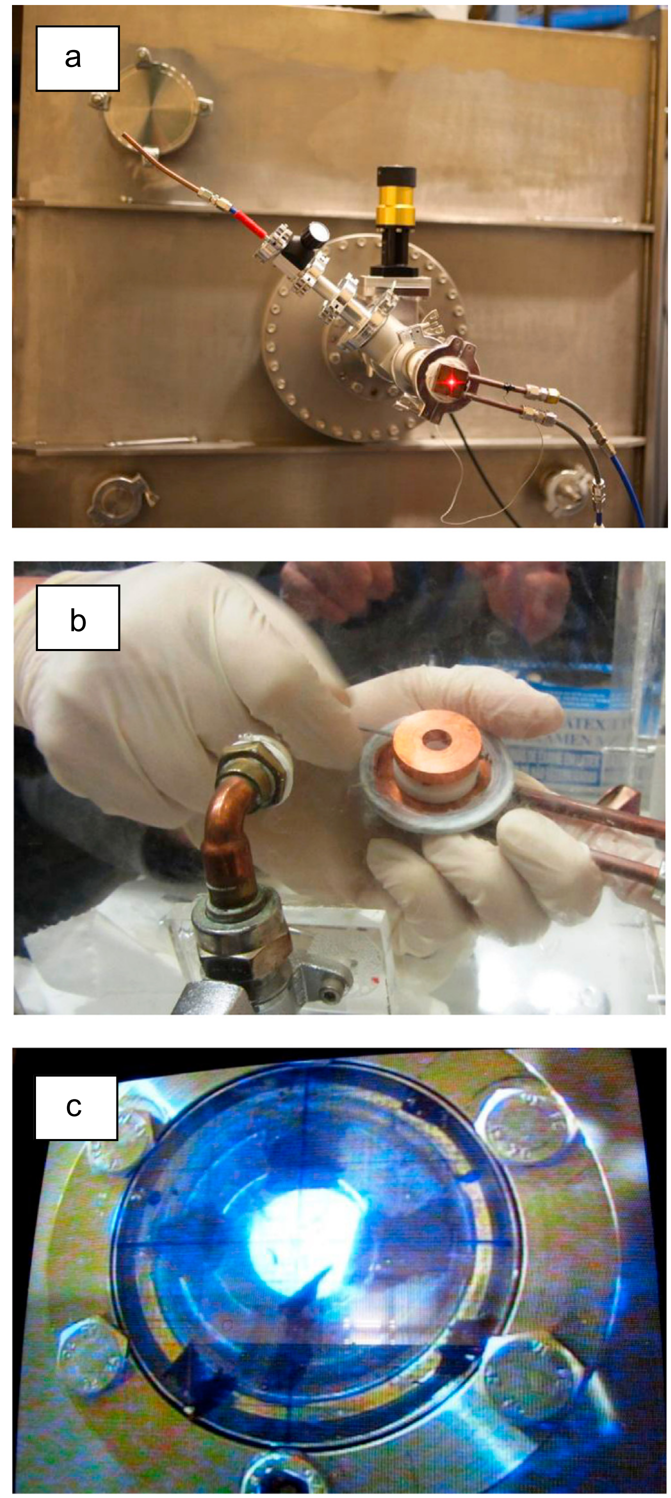

Fig. 4. (a) Experimental setup at the 3 MV Tandem Pelletron accelerator at CNA (Seville), (b) copper-Teflon® disc used to estimate the current directly reaching the lithium target (blurred of the image is due to the fact that target has to be manipulated inside an Argon chamber to avoid lithium oxidation) and (c) monitor screen detail of the neutron beam collimated in the ViewPort.

Beam focusing (Fig. 4c) was checked using a ViewPort[2] (DN 40 CF) device coupled with a luminescent quartz screen.

[2] https://www.pfeiffer-vacuum.com/productPdfs/420GSG040.en.pdf

3. Measurement results

Measurements were performed during 3 different days. Every day, the accelerator setup (focalization, energy and proton current values) was fixed. In this phase, *TNRD* reading was observed as a function of the nominal proton energy, allowing to identify the reaction threshold (1880 keV) and to verify the energy calibration of the accelerator. Energy was then increased to the project value of 1912 keV. The proton current was tuned to achieve values of thermal neutron fluence in the order of $2 \times 10^3\ \mathrm{cm^{-2}\ s^{-1}}$. The three series of 15 min measurements performed in this condition are shown in Fig. 5. For every measurement, the 15 min-time-integrated reading of the *TNRD* (termed *TNRD*) and of the proton current monitor (termed *Q*) were collected. The ratio between these two quantities, termed TNRDn, is the normalized *TNRD* reading. These quantities are reported in Table 1 for all measurements. The column $s_{\%}$ reports the standard deviation of the measurements collected during each day. As expected, $s_{\%}$ values for *Q* are slightly lower than for *TNRD*, meaning that the proportionality between proton current and thermal neutron fluence rate at the point is slightly perturbed by other beam-related sources of influence (positioning, focus, energy constancy). The impact of these sources of influence on the beam reproducibility may be estimated from the values of $s_{\%}$ for TNRDn. These values, $\pm 3.5\%$, $\pm 2.2\%$ and $\pm 1.7\%$, have been corrected by subtracting in quadrature the *TNRD* reproducibility ($\pm 1.2\%$), obtaining $\pm 3.3\%$, $\pm 1.9\%$ and $\pm 1.2\%$. Every measurement day is characterized by a different average value of TNRDn (1.24, 1.31 and 1.21), indicating that each time the accelerator is turned on and regulated, a slightly different point of work is achieved. Thus, the global inter-day uncertainty obtained for the thermal neutron beam is $\pm 4.0\%$, taking into account *TNRD* reproducibility. The availability of a reliable thermal neutron monitor, in parallel to the proton current measuring device, will be a mandatory condition to achieve reproducible irradiation conditions on this thermal neutron field. When irradiating generic devices in routine condition, the thermal neutron detector could be permanently positioned at a given angle from the target (different from 0°), or embedded in the moderating block, in order not to perturb the device under test. This would allow providing the exact value of thermal fluence delivered to a sample during a given exposure, with uncertainties comparable with the *TNRD* reproducibility.

Rough estimation of the thermal field homogeneity was performed with additional acquisitions by shifting the *TNRD*, 3 mm vertically and, successively, 3 mm laterally, from the conventional point of test. This shift was much larger than the positioning uncertainty guaranteed by the laser-based alignment system (< 1 mm). The corresponding TNRDn values differed by less than 1% from the value at the point of test.

An additional test was performed by rotating the *TNRD* of about $\pm 20°$. The observed decrease in the TNRDn value was about 7%, fully coherent with a cosine correction with angle 20°. this indicates that the angular distribution of the emitted thermal neutrons is nearly monodirectional. It is therefore clear that a good detector orthogonality is crucial for reproducible irradiation condition.

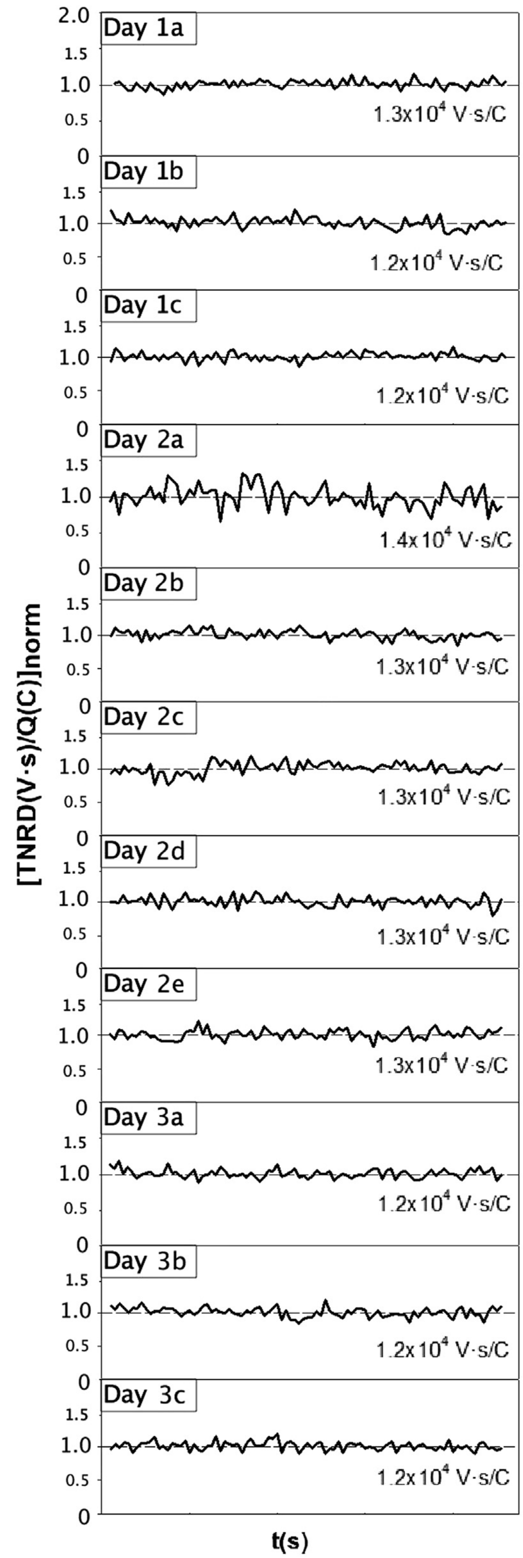

Fig. 5. On-line monitoring of the normalized ratio (signal in V s per accumulated charge in C) due to thermal neutron fluence for each measurement. The number in the right part of each graphic represents the global ratio among the whole measurement.

4. Conclusions

A thermal neutron test facility was achieved at the 3 MV Tandem Pelletron accelerator at CNA. A specific combination on proton energy, target thickness, lead shield and polyethylene moderator was studied to achieve an almost pure, photon-free, thermal field at the conventional point of test. Values of thermal neutron fluence rate up to $2 \times 10^3\ \mathrm{cm^{-2}\ s^{-1}}$ can be easily achieved. The reproducibility of the thermal neutron beam was estimated in $\pm 4\%$, over three days of operation, using a proton current integrator fixed on the target backing, and a *TNRD*-type miniaturized thermal neutron detector placed at the point of test. As expected, the proportionality between the proton current and the thermal

Table 1
TNRD readings, accumulated charge (Q) and TNRDn values along the three measurement days.

Day	Measurement	*Q* (mC)	$s_{\%}$ (%)	*TNRD* (V s)		TNRDn (V s/mC)	
1	1	15.3		19.8		1.29	
	2	13.6	9.7	16.7	13%	1.22	3.5%
	3	12.7		15.3		1.21	
2	1	15.9		21.4		1.35	
	2	13.9		18.5		1.33	
	3	13.3	7.9	17.2	10%	1.29	2.2%
	4	13.6		17.4		1.28	
	5	13.2		17.1		1.30	
3	1	14.9		18.3		1.23	
	2	14.2	2.5	16.9	3.9%	1.19	1.7%
	3	14.8		17.8		1.20	

neutron fluence rate, is perturbed by a complex set of beam-dependent factors of influence. These factors limit to about $\pm 3\%$ the reproducibility of the thermal field at the point of test. However, this facility can still be used to deliver accurate values of thermal neutron fluence, if a thermal neutron detector is permanently adopted in parallel to the proton current monitor. Embedding this detector in the moderator, in a peripheral position with respect to the 0° direction, would constitute a convenient option. Additional experiments are planned to (a) estimate the overall accuracy of the delivered thermal neutron fluence with a couple of *TNRD*s, one embedded in the moderator (monitor) and another at the point of test, (b) evaluate the spatial homogeneity of the thermal field over the whole area of the moderating plate, (c) measure the associated photon field with a reference instrument calibrated in air-kerma, and (d) establish metrologic traceability to a primary metrology Institute, for the value of thermal neutron fluence rate. After completing these actions, the studied field could be used in practice as thermal neutron calibration facility. Main advantages of this facility are:

- The spectral purity, meaning that the field is not contaminated by fast neutrons;
- Absence of radioactive sources, with considerably less safety problems with respect to radionuclide-based thermal fields.
- The installation of a continuous beam monitor will allow to use the facility with both rate-meter type or integration-type detectors.

Acknowledgments

This work would not be possible without the financial support of the CSN (Consejo de Seguridad Nuclear), Junta de Andalucía (FQM-8229), Mineco (FPA2013-47327-C2-1-R) and CEI-Biotic Granada (P-BS-64). The authors thank Juan Manuel Macarro for his inestimable technical help in the construction of the collimator and the assembly of the setup. They also wish to express their gratitude to the CNA staff, in special to Juan Angel Labrador and Angel Jesús Romero, for the high quality of the provided proton beam and their help during the experiments. They would also like to acknowledge the help provided by R. Chamorro and L. Hidalgo from the *Electromedicine department* of *HUMV*. TNRD detector was manufactured within the INFN projects NESCOFI@BTF and NEURAPID (Commissione Scientifica 5, INFN Italy).

References

Bedogni, R., Bortot, D., Introini, M.V., Gentile, A., Esposito, A., Gómez-Ros, J.M., Palomba, M., Gross, A., 2014. A new active thermal neutron detector. Radiat. Prot. Dosim. 161 (1–4), 241–244.

Expósito, M.R., Sánchez-Nieto, B., Terrón, J.A., Domingo, C., Gómez, F., Sánchez-Doblado, F., 2013. Neutron contamination in radiotherapy: estimation of second cancers based on measurement in 1377 patients. Radiother. Oncol. 107, 234–241.

Gómez, F., Iglesias, A., Sánchez-Doblado, F., 2010. A new active method for the measurement of slow-neutron fluence in modern radiotherapy treatment rooms. Phys. Med. Biol. 55, 1025–1039.

Irazola, L., Lorenzoli, M., Bedogni, R., Pola, A., Terrón, J.A., Sánchez-Nieto, B., Expósito, M.R., Lagares, J.I., Sansaloni, F., Sánchez-Doblado, F., 2014. A new online detector for estimation of peripheral neutron equivalent dose in organ. Med. Phys. 41, 112105.

Irazola, L., Terrón, J.A., Bedogni, R., Lorenzoli, M., Pola, A., Sánchez-Nieto, B., Sánchez-Doblado, F., 2015a. Signal photon component of a new thermal neutron detector TNRD in radiotherapy environments. Radiother. Oncol. 115 (1), S870 (EP-1589).

Irazola, L., Terrón, J.A., Bedogni, R., Lorenzoli, M., Pola, A., Sánchez-Nieto, B., Sánchez-Doblado, F., 2015b. TNRD neutron detector signals for different gantry angles in 6 and 15 MV. Radiother. Oncol. 115 (1), S761 (EP-1410).

Irazola, L., Terrón, J.A., Sánchez-Nieto, B., Bedogni, R., Gómez, F., Sánchez-Doblado, F., 2015c. Effects of cable extension and photon irradiation on TNRD neutron detector in radiotherapy. WC 2015, IFMBE Proccedings 51/IV, Berlin, Springer, pp. 645–649.

Lacoste, V., 2007. Design of a new IRSN thermal neutron field facility using Monte-Carlo simulations. Radiat. Prot. Dosim. 126 (1–4), 58–63.

Lederer, C., Käppeler, F., Mosconi, M., Nolte, R., Heil, M., Reifarth, R., Schmidt, S., Dillmann, I., Giesen, U., Mengoni, A., Wallner, A., 2012. Definition of a standard neutron field with the ^{7}Li(p,n)^{7}Be reaction. Phys. Rev. C 85, 055809.

Lee, C.L., Zhou, X.-L., 1999. Thick target neutron yields for the ^{7}Li(p,n)^{7}Be reaction near threshold. Nucl. Instrum. Methods Phys. Res., Sect. B 152, 1–11.

Muller, H., Gressier, V., Lacoste, V., Lebreton, L., Pochat, J.-L., 2003. Characterization of the Thermal Neutron Field Produced by the IRSN Sigma Facility. 9. Abstract book Neudos, Delft, The Netherlands.

Pelowitz, D.B., 2005. MCNPX Users Manual Version 2.5.0-LA-CP05-0369. Los Alamos National Laboratory LACP, USA.

Praena, J., Mastinu, P.F., Pignatari, M., Quesada, J.M., García-López, J., Lozano, M., Dzysiuk, N., Capote, R., Martín-Hernández, G., 2013. Measurement of the MACS of 181Ta(n,γ) at kT=30 keV as a test of a method for Maxwellian neutron spectra generation. Nucl. Instrum. Methods Phys. Res. 727, 1–6.

Praena, J., Mastinu, P.F., Pignatari, M., Quesada, J.M., Capote, R., Morilla, Y., 2014. Measurement of the MACS of 159Tb(n,γ) at kT= 30 keV by activation. Nucl. Data Sheets 120, 205–207.

Praena, J., Irazola, L., Fernández, B., Terrón, J.A., Bedogni, R., Lorenzoli, M., Pola, A., Sánchez-Nieto, B., Sánchez-Doblado, F., 2015. Proposal of thermal neutron detector stability for peripheral dose estimation in clinic at a novel neutron facility. Radiother. Oncol. 115 (1), S735 (EP-1365).

Romero-Expósito, M.R., Sánchez-Nieto, B., Terrón, J.A., Lopez, M.C., Ferreira, B.C., Grishchuk, D., Sandíns, C., Moral-Sánchez, S., Bragado-Álvarez, L., Melchor, M., Domingo, C., Gómez, F., Sánchez-Doblado, F., 2015. Comminsioning the neutron production of a linac: development of a clinical planning tool for second cancer risk estimation. Med. Phys. 42, 276–281.

Sánchez-Doblado, F., Domingo, C., Gómez, F., Sánchez-Nieto, B., Muñiz, J.L., García-Fusté, M.J., Expósito, M.R., Barquero, R., Hartmann, G., Terrón, J.A., et al., 2012. Estimation of neutron equivalent dose in organs of patients undergoing radiotherapy by the use of a novel online digital detector. Phys. Med. Biol. 57, 6167–6191.

Terrón, J.A., Irazola, L., Morilla, Y., Muñiz, G., Bedogni, R., Lorenzoli, M., Pola, A., Sánchez-Nieto, B., Sánchez-Doblado, F., 2015. Photon energy response of TNRD neutron detector in a ^{60}Co irradiator and a 6 MV clinic. Radiother. Oncol. 115 (1), S757–S758 (EP-1404).

Yu, W., Yue, G., Han, X., Chen, J., Tian, B., 1998. Measurements of the neutron yields from ^{7}Li(p,n)^{7}Be reaction (thick target) with incident energies from 1.885 to 2.0 MeV. Med. Phys. 25 (7 Pt 1), 1222–1224.